

Quantum Chaos on Graphs

Tsampikos Kottos and Uzy Smilansky

Department of Physics of Complex Systems, The Weizmann Institute of Science, Rehovot 76100, Israel
(Received 22 July 1997)

We quantize graphs (networks) which consist of a finite number of bonds and nodes. We show that their spectral statistics is well reproduced by random matrix theory. We also define a classical phase space for the graph, where the dynamics is mixing and the periodic orbits (loops on the graph) proliferate exponentially. An exact trace formula for the quantum spectrum is developed and used to investigate the origin of the connection between random matrix theory and the underlying chaotic classical dynamics. Being an exact theory, and due to its relative simplicity, it offers new insights into this problem which is at the forefront of the research in quantum chaos and related fields. [S0031-9007(97)04707-8]

PACS numbers: 05.45.+b, 03.65.Sq

Quantized graphs (networks) were used frequently to model systems of interest in quantum chemistry [1], solid state physics [2], and transmission of waves [3]. The mathematical properties of the Schrödinger operator on graphs were also investigated [4,5]. We cannot do justice to all the previous studies. Rather, we cite a few review papers or representative works, where further bibliographies can be found. Our main purpose is to show that quantum graphs provide a simple model which displays most of the phenomena encountered in quantum systems which are chaotic in the classical limit. In particular, the generic spectral statistics displayed by quantum graphs can be investigated in detail, and its origin is traced to specific topological properties of the classical periodic orbits.

Graphs consist of V vertices connected by bonds. The connectivity matrix $C_{i,j}$, $i, j = 1, \dots, V$ takes the value 1 if the vertices i and j are connected by a bond, and 0 otherwise. The valency of a vertex is given by $v_i = \sum_{j=1}^V C_{i,j}$ and the total number of directed bonds is $2B = \sum_{i,j=1}^V C_{i,j}$. We denote by $b = (i, j)$ the bond directed from i to j , and \hat{b} its reverse (j, i) . The positive direction on the bond $b = (i, j)$ points from $\min(i, j)$ to $\max(i, j)$. As will be shown below, the topological characterization of the graph which was given above is sufficient for the study of "classical dynamics" on graphs. For the quantum description we need the metric information, namely, the lengths of the bonds L_b , $b = 1, \dots, 2B$ and $L_b = -L_{\hat{b}}$. To avoid degeneracies we shall henceforth assume that the L_b are not rationally related.

The Schrödinger operator is defined on the graph in the following way [4]: On each bond the wave function is a solution of the one-dimensional equation

$$\left(-i \frac{d}{dx} - A\right)^2 \Psi_b(x) = k^2 \Psi_b(x), \quad (1)$$

where $\text{Re}(A) \neq 0$ breaks time reversal symmetry. At each vertex, the wave function must be uniquely defined. The conservation of the probability current is imposed by the boundary conditions (Neumann) [4]

$$\sum_{j=1}^{v_i} \left(-iA + \frac{d}{dx}\right) \Psi_{ij}(x) \Big|_{x=0} = 0. \quad (2)$$

This set of boundary conditions ensures that the Schrödinger operator is self-adjoint, and hence the existence of an unbounded, discrete spectrum of real wave numbers $\{k_n\}$ for which a nontrivial solution exists.

The secular equation for the quantized graph [4] can be solved numerically to provide an arbitrarily large sequence of eigenvalues. The resulting (integrated) nearest neighbor distributions for the fully connected square (tetrahedron) with $A = 0$ and $A \neq 0$ are shown in Fig. 1 together with the predictions of random matrix theory (RMT) for the GOE and GUE ensembles. We made similar comparisons for other simple graphs and observed the same degree of agreement. Thus, we face an exceedingly simple class of systems which belongs to the same spectral universality class as quantum systems which are chaotic in the classical limit. We shall show that quantum graphs share many properties with generic quantum Hamiltonians, and their simplicity enables us to get new

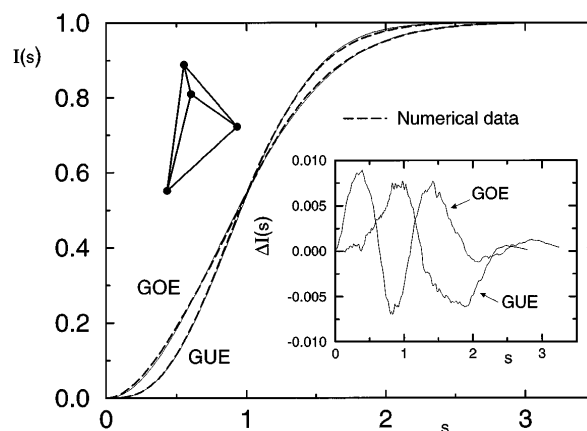


FIG. 1. Integrated nearest neighbor distribution based on the lowest 80 000 levels of a single realization of a tetrahedron. ΔI indicates the deviation from the RMT results.

understanding of the connection between RMT and quantum chaos.

The matching conditions (2) can be translated into vertex scattering matrices, which provide a unitary transformation between the outgoing and incoming waves at each vertex. The $v_i \times v_i$ scattering matrix at the i th vertex is

$$\sigma_{ji,ij'}^{(i)} = \left(-\delta_{j,j'} + \frac{2}{v_i}\right) C_{i,j} C_{i,j'}. \quad (3)$$

Note that backscattering is singled out both in magnitude and sign. Scattering from a “dead-end” vertex ($v_i = 1$) is trivial since $\sigma_{ji,ij}^{(i)} = 1$. The secular equation is obtained by imposing a consistency condition on the wave functions on all the bonds: a wave which is an *outgoing wave* from i to j appears also as an *incoming wave* at j with the appropriate phase. This can be translated into a secular equation of the form [5]

$$Z(k, A) = \det[I - S(k, A)] = 0. \quad (4)$$

Here, the graph “scattering matrix” $S(k, A) = D(k; A)T$ is a unitary matrix in the $2B$ dimensional space of directed bonds. It is a product of a diagonal unitary matrix $D(k, A)$ which depends on the metric properties of the graph, and a constant orthogonal matrix T which depends exclusively on the topology.

$$\begin{aligned} D_{ij,i'j'}(k, A) &= \delta_{i,i'} \delta_{j,j'} e^{ik|L_{ij}| + iAL_{ij}}, \\ T_{ji,nm} &= \delta_{n,i} C_{j,i} C_{i,m} \sigma_{ji,im}^{(i)}. \end{aligned} \quad (5)$$

The spectral counting function $N(k)$ is given by [6]

$$N(k) = \bar{N}(k) + \frac{1}{\pi} \operatorname{Im} \sum_{n=1}^{\infty} \frac{1}{n} \operatorname{tr}[S(k)]^n, \quad (6)$$

where

$$\bar{N}(k) - \bar{N}(0) = \frac{1}{2\pi} \{\det[-S(k)] - \det(-T)\} = \frac{k\mathcal{L}}{2\pi}. \quad (7)$$

Here $\mathcal{L} = 2\sum_{b=1}^B L_b$ is twice the total length of the graph. The mean level density $\bar{d} = \partial_k \bar{N}(k)$ is independent of k and $\bar{N}(0) = 1/2$. The Heisenberg length is also constant ($l_H = 2\pi\bar{d} = \mathcal{L}$). This is a peculiarity of systems in one dimension, which will be of great importance in the following. The oscillatory part of the counting function is expressed in terms of $\operatorname{tr}[S(k)]^n$. The latter are given as sums over periodic loops of period n on the graph:

$$\operatorname{tr}[S(k)]^n = \sum_{p \in P_n} n_p g_p A_p^r e^{(ikl_p + iAb_p)r} e^{ir\mu_p\pi}, \quad (8)$$

where the sum is over the set P_n of primitive periodic orbits whose period n_p is a divisor of n , which $r = n/n_p$. Periods which are related by exact symmetry are counted once, and their multiplicity g_p appears explicitly. l_p and b_p are the length and the directed length, respectively, and

the stability factors are given by

$$A_p = \prod_{s=1}^{\mu_p} \left| \left(1 - \frac{2}{v_s}\right) \right| \prod_{t=1}^{v_p} \frac{2}{v_t} \equiv e^{-\frac{\lambda_p}{2} n_p}. \quad (9)$$

Here μ_p is the number of vertices where nontrivial ($v_s \neq 1$) backscattering occurs. At the other v_p vertices on the loop the scattering is not backwards, and $n_p - (\mu_p + v_p) \geq 0$. λ_p plays the role of the Lyapunov exponent. Substituting (8) into (6) and taking the derivative with respect to k one gets an exact trace formula

$$\begin{aligned} d(k) &= \sum_{n=1}^{\infty} \delta(k - k_n) \\ &= \frac{\mathcal{L}}{2\pi} + \frac{1}{\pi} \sum_{p,r} \frac{l_p g_p \cos r(kl_p + Ab_p + \mu_p\pi)}{e^{\frac{\lambda_p}{2} n_p r}}. \end{aligned} \quad (10)$$

It bears a striking formal similarity to the well known exact and semiclassical trace formulas for chaotic Hamiltonian systems [7,8]. In particular, the number of n -periodic loops on the graph is $\frac{1}{n} \operatorname{tr} C^n$, where C is the connectivity matrix. Since its largest eigenvalue is proportional to the mean valency $\bar{v} = 2B/V$, periodic loops proliferate exponentially with topological entropy $\approx \log \bar{v}$. The vertex labels, together with the connectivity matrix, provide a symbolic (Bernoulli) dynamics on the graph. The stability amplitudes decrease exponentially with n but not enough to make the series for $d(k)$ absolutely convergent (positive entropy barrier). Finally, μ_p is the analog of the Maslov index. Its origin is topological, and it counts the number of times nontrivial backscattering occurs along the loop.

At this stage it is appropriate to introduce the classical analog of the quantum graph. Classical trajectories can be easily defined on the bonds, but not on the vertices which are singular points. However, we can construct a Poincaré section by registering at each crossing of a vertex the direction at which the particle points. The set of all possible vertices and directions is equivalent to the set of $2B$ directed bonds. The evolution on this Poincaré section is well defined once we postulate the transition probabilities $U_{b,b'}$ between the bonds b, b' at a vertex. The quantum $S(k, A)$ matrix provides the desired probabilities via $U_{b,b'} = |S_{b,b'}(k; A)|^2 = |T_{b,b'}|^2$. Note that $U_{b,b'}$ does not involve any metric information on the graph. The unitarity of the graph scattering matrix guarantees $\sum_{b=1}^{2B} U_{b,b'} = 1$, so that the number of classical particles is conserved during the evolution. If $\rho_b(t)$ denotes the probability to occupy the bond b at the (topological) time t , then

$$\rho_b(t+1) = \sum_{b'} U_{b,b'} \rho_{b'}(t). \quad (11)$$

This is a Markovian master equation for the classical density and the matrix $U_{b,b'}$ is the evolution (Frobenius-Peron) operator. The largest eigenvalue in the spectrum of U is 1, and the corresponding eigenvector describes a uniform

distribution (equilibrium). The other eigenvalues are inside the unit circle, and therefore the system reaches the uniform distribution exponentially fast. This is characteristic of a classically mixing system. Of prime importance in the discussion of the relation between the classical and the quantum dynamics are the traces $u_n = \text{tr}(U^n)$ which are interpreted as the mean classical probability to perform n -periodic motion. Recalling $u_n \xrightarrow{n \rightarrow \infty} 1$, one obtains a classical sum rule by substituting the periodic orbit expansion of u_n ,

$$u_n = \sum_{p \in P_n} n_p g_p (|A_p|^2)^r \xrightarrow{n \rightarrow \infty} 1. \quad (12)$$

Each periodic orbit is endowed with a weight $|A_p|^2$ defined in terms of the stability amplitudes (9). It is the probability to remain on the orbit. These weights are the counterparts of the stability weights $|\det(I - M_p)|^{-1}$ for hyperbolic periodic orbits in Hamiltonian systems, where M_p is the monodromy matrix. Graphs, however, are one dimensional and the motion on the bonds is simple and stable. Ergodic (mixing) dynamics is generated, however, because at each vertex a (Markovian) choice is one out of ν directions is made. Thus, chaos on graphs originates from the multiple connectivity of the (otherwise linear) system. The morphology of periodic orbits undergoes a transition at $n \approx 2B$. From the topological point of view, all the periodic orbits become composites of irreducible loops whose period is less than $2B$. Metric degeneracies become also abundant, even though the lengths of the bonds are assumed to be incommensurate. It is interesting to note that when the quantum wave numbers are measured in units of the inverse mean bond length, the Heisenberg length $l_H = \mathcal{L}$ equals $2B$.

As a prelude to the study of the spectral statistics of a graph, we shall investigate the *circular* ensemble of the $S(k, A)$ matrices of the graph. Because of (4) the statistical properties of the spectrum of the $2B$

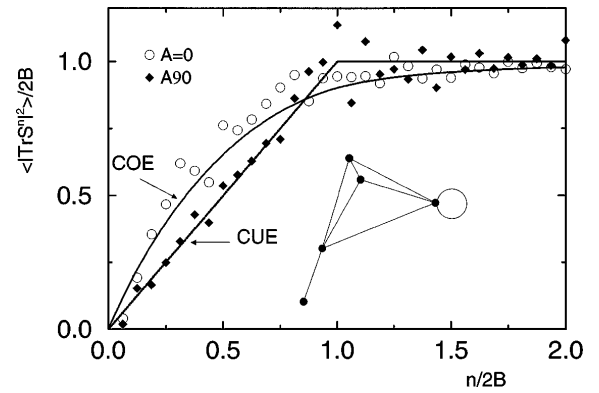


FIG. 2. The form factors $\frac{1}{2B} \text{tr}[S(k)]^n$ for the tetrahedron with one dangling line and a loop.

eigenphases of S will be reflected in the energy spectral statistics. The ensemble is generated by averaging over k (and also over A with $\langle A \rangle \neq 0$ when time reversal symmetry is broken). Since the dimension of S is independent of k and of A , one can choose arbitrarily large averaging intervals for this purpose. We computed $\frac{1}{2B} \langle |\text{tr} S^n|^2 \rangle$ which is the form factor for the two point correlation function of the eigenphases spectrum. It agrees quite well with the predictions of RMT (Fig. 2).

To investigate further the dynamical origins of the rigidity (see Fig. 1), we study the two point form factor

$$K(\tau; \bar{k}) = \frac{1}{\mathcal{N}} \left| \sum_{|k_n - \bar{k}| \leq \Delta_k/2} e^{i 2\pi k_n \mathcal{L} \tau} \right|^2 - \mathcal{N} \delta(\tau), \quad (13)$$

where we consider a spectral interval of size Δ_k , centered about \bar{k} and involving $\mathcal{N} = \bar{d} \Delta_k$ eigenvalues. τ measures lengths in units of the Heisenberg length $l_H = \mathcal{L}$. We consider first the case $A = 0$. Splitting $K(\tau; \bar{k})$ to its diagonal $[K_D(\tau, \bar{k})]$ and nondiagonal parts $[K_{ND}(\tau, \bar{k})]$, we write them in terms of periodic orbits

$$K_D(\tau, \bar{k}) = \frac{2\mathcal{N}}{\mathcal{L}^2} \sum_{p,r} |\tilde{A}_p^r|^2 \left[\delta_{\mathcal{N}} \left(\frac{r l_p}{\mathcal{L}} - \tau \right) \right]^2, \\ K_{ND}(\tau, \bar{k}) = \frac{2\mathcal{N}}{\mathcal{L}^2} \sum_{p,r \neq p',r'} \tilde{A}_p^r \tilde{A}_{p'}^{r'} e^{i\pi(r\mu_p - r'\mu_{p'})} \delta_{\mathcal{N}} \left(\frac{r l_p}{\mathcal{L}} - \tau \right) \delta_{\mathcal{N}} \left(\frac{r' l_{p'}}{\mathcal{L}} - \tau \right) \cos \bar{k}(r l_p - r' l_{p'}), \quad (14)$$

where we use $\tilde{A}_p = n_p l_p g_p A_p$ and $\delta_{\mathcal{N}}(x) = \sin \frac{\mathcal{N}x}{2} / \frac{\mathcal{N}x}{2}$. K_D is a classical expression, because all interference effects are neglected, but for the ones which are due to exact symmetries. The sum rule (12) enables us to justify a Hannay and Ozorio De Almeida-like sum rule [9], from which it follows that $K_D(\tau) \approx \langle g \rangle \tau$ [10]. For $\tau \ll 1$ $K(\tau) \approx K_D(\tau)$. Because of the fact that the quantum spectrum is real and discrete, $K(\tau)$ must approach 1 for $\tau > 1$. This is taken care of by K_{ND} . In contrast to the diagonal part, K_{ND} depends crucially on the phase correlations between the contributing terms.

In Hamiltonian systems in more than one dimension, the size of the spectral interval Δ_k is limited by the requirement that the smooth spectral density is approximately constant. Here \bar{d} is constant; hence one can take arbitrarily large Δ_k to make the $\delta_{\mathcal{N}}(x)$ arbitrarily narrow. In Fig. 3 we show the numerical $K(\tau)$ calculated with two extreme values of \mathcal{N} .

As long as $\tau \mathcal{L}$ is shorter than the length of the shortest period orbit, $K(\tau) = 0$. Beyond this point, the low resolution curve does not deviate much from the prediction of

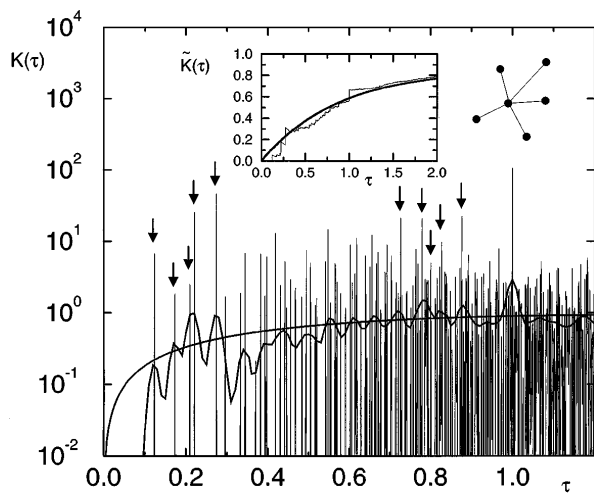


FIG. 3. Two point form factor for the five star graph ($\approx 100\,000$ levels). The arrows indicate the location of the short periodic orbits and their reciprocal lengths with respect to the Heisenberg length.

RMT, and it saturates at 1 when $\tau > 1$. We shall explain the residual structure in the sequel. The high resolution data show a similar behavior, which can be better checked if one studies $\bar{K}(\tau) = \frac{1}{\tau} \int_0^\tau K(t) dt$ (see inset). However, by increasing the resolution, correlations between periodic orbits with different lengths are suppressed, and the interference mechanism which builds up K_{ND} cannot be due to the correlations in the spectrum of periodic orbit lengths, but to another source: For $\tau > 1/2$ the periodic orbits must traverse some bonds more than twice. The likelihood of periodic orbits which traverse the same edges the same number of times but with different backscatter indices μ_p is increasing, and the interferences which build K_{ND} are due to the sign correlations among orbits of exactly the same lengths (when $A \neq 0$ one has to restrict the discussion to loops with the same directed length). The distribution of backscatter indices of periodic orbits is a problem that was not yet addressed by probabilistic graph theory. Our numerical results together with the general experience from quantum chaos allow us to conjecture that the spectral form factor connects RMT with the distribution of backscatter indices on loops.

Finally, the structure observed in the function $K(\tau)$, decorating the rather smooth background, can be attributed to low τ to the short and rather scarce periodic orbits. The arrows in the figure indicate their location. The structures near $\tau = 1$ reproduce a trend which was predicted on different grounds in [11], namely, the spikes appear at lengths $\mathcal{L} - l_p$ (see arrows in Fig. 3). We can explain this phenomenon with the help of Newton's iden-

ties which relate $\text{tr}[S(k)]^n$ to the coefficients of the characteristic polynomial, and the inversive symmetry of the latter [12]. Simple algebra gives

$$\sum_{n=1}^B \frac{\text{tr} S^{2B-n}}{2B-n} = e^{i\mathcal{L}k+\phi_0} \sum_{n=1}^B \frac{(\text{tr} S^n)^*}{n} + \dots, \quad (15)$$

where the phase ϕ_0 is independent of k and \dots stands for terms which involve amplitudes and phases of composite orbits. Substituting (8) and taking the Fourier transform, we find that the contributions of the terms $\text{tr} S^{2B-n}$ to the length spectrum appear at lengths $\mathcal{L} - l_p$, where l_p are lengths associated with the shorter periodic orbits with periods n .

Because of lack of space we are not able to discuss some more results and possible experimental demonstrations. The wealth of problems which have their counterparts in graphs, and the lessons they can teach are far from being exhausted.

This research was supported by the Minerva Center for Physics of Nonlinear Systems, and by a grant from the Israel Science Foundation.

-
- [1] M. J. Richardson and N. L. Balazs, *Ann. Phys. (N.Y.)* **73**, 308 (1971).
 - [2] Y. Avishai, Y. Hatsugai, and M. Kohmoto, *Phys. Rev. B* **47**, 9561 (1993); T. Nakayama, K. Yakubo, and R. L. Orbach, *Rev. Mod. Phys.* **66**, 381 (1994).
 - [3] P. Exner and R. Gawlista, *Phys. Rev. B* **53**, 7275 (1996); P. Exner, *Phys. Rev. Lett.* **74**, 3503 (1995); C. Flesia, R. Johnston, and H. Kunz, *Europhys. Lett.* **3**, 497 (1987).
 - [4] J. E. Avron, in *Proceedings of the 1994 Les Houches Summer School on Mesoscopic Quantum Physics*, edited by E. Akkermans *et al.* (North-Holland, Amsterdam, 1995), pp. 741–791.
 - [5] R. Carlson, “Inverse Eigenvalue Problems on Directed Graphs” (to be published).
 - [6] U. Smilansky, in *Proceedings of the 1994 Les Houches Summer School on Mesoscopic Quantum Physics* (Ref. [4]).
 - [7] A. Selberg, *J. Ind. Math. Soc.* **20**, 47 (1956).
 - [8] M. G. Gutzwiller, in *Chaos in Classical and Quantum Mechanics*, *Interdisciplinary Applied Mathematics Vol. 1*, edited by F. John (Springer-Verlag, New York, 1990).
 - [9] J. H. Hannay and A. M. Ozorio De Almeida, *J. Phys. A* **17**, 3429 (1984).
 - [10] M. V. Berry, *Proc. R. Soc. London A* **400**, 229 (1985).
 - [11] E. B. Bogomolny and J. P. Keating, *Phys. Rev. Lett.* **77**, 1472 (1996); O. Agam *et al.*, *ibid.* **75**, 4389 (1995).
 - [12] F. Haake, M. Kus, H.-J. Sommers, H. Schomerus, and K. Zyczowski, *J. Phys. A* **29**, 3641 (1996).